

**Influence of pinning effects on the ferroelectric hysteresis in cerium-doped  $\text{Sr}_{0.61}\text{Ba}_{0.39}\text{Nb}_2\text{O}_6$** 

T. Granzow, U. Dörfler, and Th. Woike

*Institut für Kristallographie, Universität zu Köln, Zùlpicherstrasse 49b, D-50674 Köln, Germany*

M. Wöhlecke, R. Pankrath, and M. Imlau

*Fachbereich Physik, Universität Osnabrück, Barbarastrasse 7, D-49069 Osnabrück, Germany*

W. Kleemann

*Laboratorium für Angewandte Physik, Gerhard-Mercator-Universität Duisburg, Lotharstrasse 65, D-47048 Duisburg, Germany*

(Received 19 September 2000; published 26 March 2001)

The temporal behavior of ferroelectric domains under external electric field is investigated in cerium-doped strontium-barium-niobate crystals using quasistatic surface-charge detection. The polarization reversal depends strongly on frequency, temperature, dark conductivity, and doping concentration. This so-called *electrical aging* is attributed to electric pinning centers that hinder the domain-wall motion. We discuss the existence of pinning centers on the basis of the quenched random-field model.

DOI: 10.1103/PhysRevB.63.174101

PACS number(s): 77.80.Fm, 77.22.Ej, 77.80.Dj, 77.84.Dy

**I. INTRODUCTION**

The relaxor ferroelectric strontium-barium-niobate  $\text{Sr}_x\text{Ba}_{1-x}\text{Nb}_2\text{O}_6$  (SBN) is a nearly ideal material for fundamental research of relaxor-type phase transitions, ferroelectric domains, and their dynamical behavior. This is due to physical effects with large parameters such as pyro- and piezoelectric coefficients,<sup>1</sup> spontaneous polarization,<sup>2</sup> and linear electro-optical constants.<sup>3</sup> Furthermore, striation-free crystals of the congruently melting composition with  $x=0.61$  (SBN61) can be grown with high purity.

SBN61 is a typical representative of tetragonal unfilled tungsten-bronze-type compounds. Within the tetragonal system it undergoes a relaxor phase transition from the ferroelectric low-temperature phase (point group  $4mm$ ) into the para-electric high-temperature phase ( $4/mmm$ ).<sup>4-6</sup> In the ferroelectric phase, the crystal contains needlelike  $180^\circ$  domains parallel to the crystallographic  $c$  axis, allowing only two equivalent polarization directions.<sup>7</sup> This system of polar symmetry can best be described by an Ising-like model.<sup>8</sup> Due to the incommensurate structure the local site symmetry is lowered to orthorhombic.<sup>9</sup> The transition temperature  $T_M$  (defined as the temperature maximum of the low-frequency dielectric constant) of pure SBN61 is  $T_M=350$  K, while the maximum temperature  $T_M$  of doped SBN61 is significantly lower. When doped with  $\text{Ce}^{3+}$  it decreases linearly with the doping concentration, and for concentrations of about 2 mol % and more the transition temperature drops below room temperature. The ferroelectric hysteresis of SBN61 was measured by Maciolek and Liu<sup>10</sup> using a Sawyer-Tower bridge. They found a serious recession of the ferroelectric hysteresis loop after switching several times. Aging of the polarization in SBN75, where  $x=0.75$ , was evidenced by Jimenez *et al.*,<sup>11</sup> and Xia *et al.* found that Cu doping of SBN61 prevents aging behavior.<sup>12</sup>

The phase transition in SBN is of relaxor-type, i.e., it is ‘‘smeared’’ or ‘‘diffused.’’ The order parameter, the spontaneous polarization, and all other physical parameters characteristic for crystals with no inversion center do not vanish

spontaneously at  $T_M$ . They can still be evidenced on a nanoscale in the para-electric regime. To explain this breakdown of the conventional transitional behavior a ‘‘random-field Ising model’’ as a consequence of structural or compositional inhomogeneity was introduced.<sup>13</sup> This model is based on the assumption of charge disorders giving rise to random fluctuations of the crystalline internal electric field. At high temperatures these fluctuations stabilize dynamic nanodomains, which lead to a nonzero spontaneous polarization in the para-electric phase. When the temperature is lowered below the transition temperature the domains become more and more cooperative, until a ferroelectric state is reached. The interaction between the domains leads to a characteristic dynamic behavior that influences the reaction of the system to an external electric field. The temporal behavior of the ferroelectric domains therefore gives important insight into the phase-transition process.

The purpose of this study is the investigation of the electric polarization by detecting charge carriers on the crystal surface to examine the dynamical behavior of the ferroelectric domains in the low-temperature phase. In this report we discuss investigations on the temporal behavior of the electric polarization in cerium-doped SBN61 under a constant external electric field as well as the ferroelectric hysteresis and its development measured with very low frequencies ( $<10^{-3}$  Hz). These results prove the existence of an aging effect that depends on doping, temperature, and the measuring frequency. We explain this effect on the basis of random local electric fields that influence the dynamics of the domain walls.

**II. EXPERIMENTAL SETUP**

Single crystals of tetragonal  $\text{Sr}_{0.61}\text{Ba}_{0.39}\text{Nb}_2\text{O}_6$  are grown by the Czochralski technique and cut perpendicular to the crystallographic  $c$  axis. Specimens with dimensions of  $7 \times 7$  mm<sup>2</sup> and thicknesses between 0.7–1.2 mm are polished to optical quality. In order to achieve monodomain crystals, the samples were electrically poled by first heating up to

140 °C, then applying an electric field of 350 V/mm parallel to the  $c$  axis and finally slowly cooling down to room temperature. This process is called ‘‘field cooling’’ (FC), in contrast to the zero-field-cooled (ZFC) protocol giving rise to randomly oriented 180° domains. The two  $c$  faces of the sample are connected to a computer-controlled voltage supply and a charge amplifier, respectively. The sample is fixed in a vacuum chamber that is evacuated to 1 Pa to minimize undesirable external influences on the surface charge. The electric field  $E$  applied to the sample is then raised in steps of predetermined heights and widths from 0–450 V/mm. After reaching the maximum of the electric field, it is lowered in steps down to  $-450$  V/mm before returning in steps to 0 V/mm. The cycle time of these discontinuous field changes is determined by the width, typically 5 s, and the height 2.5 V/mm of the steps. Thus a single loop lasts 3200 s, corresponding to a frequency of  $3.125 \cdot 10^{-4}$  Hz. During the whole loop the charge accumulating on the  $c$  faces of the crystal is measured by the charge amplifier. The accumulated surface charge is converted to the sample polarization  $P$  by dividing the total measured charge by the known area of the  $c$  face of the sample. The result is a very low-frequency hysteresis loop  $P(E)$ . The temporal behavior of the domain walls and the domain reversal is investigated by setting the external electric field abruptly to characteristic values of the hysteresis such as the coercive field. Domain-wall movements are measured with field-cooled crystals by setting the external field from 0–300 V/mm in the direction of the field used in the poling process. After the polarization has reached saturation, the external field is turned off, and the decay of the built-up polarization is measured. Afterwards, the domain-reversal process is examined by setting the external field to  $-300$  V/mm. During all measurements the sample temperature is kept constant within an accuracy of 0.01 °C with a temperature controller and a peltier element, thus eliminating or at least strongly suppressing the influence of the pyroelectric effect.

### III. EXPERIMENTAL RESULTS

#### Temporal behavior of domain walls and the polarization reversal

The characteristic temporal behavior of domain walls and polarization reversal is important for the understanding of the ferroelectric hysteresis. To obtain reliable hysteresis loops, the polarization has to follow the external electric field without a significant phase shift. A typical time dependence of the polarization  $P(t)$  is presented in Fig. 1. In this case, an external electric field of 300 V/mm acts as the driving force for the domains and domain walls. It is applied to a field-cooled crystal in the direction of the previously prepared polarization at 24.5 °C. The sample used is a SBN61 crystal doped with 0.66 mol % cerium. The data points have been thinned out by a factor of 200 to improve visibility. The discontinuity at the beginning of the spectrum is due to the polarization change caused by the static dielectric constant. This change happens on a time scale not accessible with our method. However, the first jump in the polarization gives

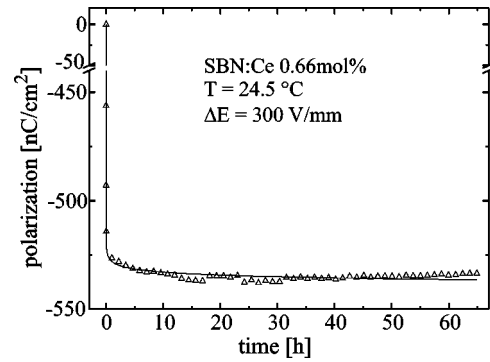


FIG. 1. Buildup of electric polarization in a poled SBN:Ce crystal with an external electric field of 300 V/mm in the primary poling direction. The points have been thinned out to allow better observation. The continuous line is the result of a fit with the KWW function, resulting in values of  $\beta=0.05\pm 0.02$  and  $\tau=(0.02\pm 0.01)$  s.

$\epsilon_{33}=1840$ , a value in good agreement with the values of  $\epsilon_{33}=1950$  obtained from low-frequency measurements.<sup>14</sup> An axis break has been inserted between  $-50$ – $-400$  nC/cm<sup>2</sup> since we obtained no data in that region. The curve presented in Fig. 1 is corrected for a small dark-current contribution, resulting in a horizontal line on a long-time scale. In the original measurement the polarization is observed to increase to a saturation state with a constant slope. This slope results from charge carriers traveling through the crystal due to its nonzero dark conductivity of  $\sigma=(2.9\pm 0.3)\times 10^{-11}$   $\Omega^{-1}\text{m}^{-1}$ . The small deviations from an ideal line are due to the influence of the pyroelectric effect, which is noticeable even though the temperature was kept constant up to 0.01 °C. The data cannot be fitted with one, two, or three simple exponentials, but can be fitted with a Kohlrausch-Williams-Watts (KWW) or stretched exponential function

$$P(t) = P_{\infty} - P \cdot \exp\left[-\left(\frac{t}{\tau}\right)^{\beta}\right], \quad (1)$$

with the stretching exponent  $\beta$  and the average lifetime  $\tau$ , resulting in  $\beta=0.05\pm 0.02$  and  $\tau=(0.02\pm 0.01)$  s. The fit is represented by the continuous line in the figure.

The relaxation of the domains and domain walls when the external field is removed is presented in Fig. 2. The observed nonexponential time dependence follows again a stretched exponential function, with the parameters  $\beta=0.087\pm 0.009$  and  $\tau=(0.02\pm 0.01)$  s. They do not differ significantly from the values obtained from the above measurement with an applied electric field. Both the buildup and the decay of the polarization occur nearly instantaneously. The small aberrations of the fit from the measured data is again due to the pyroelectric effect. The data points are once again thinned out to allow us to distinguish between measured and fitted data.

In order to determine the temporal behavior of the domain-reversal process, an external electric field of 300 V/mm is applied antiparallel to the poling direction of the field-cooled crystal. This field is about twice that of the coercive field (160 V/mm), so we can expect that the crystal

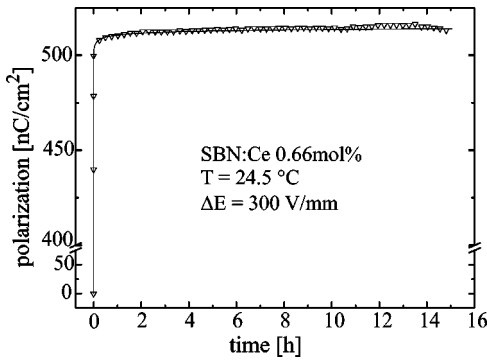


FIG. 2. Decay of electric polarization after removal of external electric field. Fitting with the KWW function results in  $\beta=0.087 \pm 0.009$  and  $\tau=(0.02 \pm 0.01)$  s.

will reverse the orientation of its electric polarization. The result is shown in Fig. 3. The polarization is saturated in less than 100 s; a fit with a stretched exponential function gives  $\beta=0.402 \pm 0.005$  and  $\tau=(1.99 \pm 0.03)$  s. The small discrepancy between fit and experimental data for  $t \leq 2$  s is due to the limited time resolution of our detector. After correction for the dark current, we measured a total polarization change of  $45.7 \mu\text{C}/\text{cm}^2$ . When the electric field is removed, a decay of the polarization very similar to that shown in Fig. 2 is observed. This second decay has a 15% larger total value ( $590 \text{ nC}/\text{cm}^2$ ) than the first one ( $515 \text{ nC}/\text{cm}^2$ ). For a fit we obtained  $\beta=0.05 \pm 0.01$  and  $\tau=(8.5 \pm 0.5)$  s, thus this decay process needs a longer time until the configuration is stabilized without an electric field.

To further investigate this indication of aging, the domains are once again switched by applying an electric field contrary to the new polarization orientation. The difference between this curve and the one shown in Fig. 3, that depicts the first repoling process is again a quantitative one. While the first repoling process resulted in a polarization change of  $45.7 \mu\text{C}/\text{cm}^2$ , this second polarization reversal renders values of only  $10.5 \mu\text{C}/\text{cm}^2$ , a reduction of about 75%. The data can be fitted with  $\tau=(9.9 \pm 0.5)$  s, which is comparable

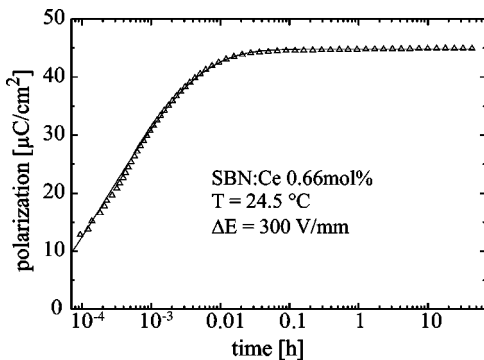


FIG. 3. Temporal behavior of the ferroelectric polarization with an external field of 300 V/mm applied contrary to the polar axis. The time axis is presented in a logarithmic scale to allow better comparison between experimental data and fit. The fit returns  $\beta=0.402 \pm 0.005$  and  $\tau=(1.99 \pm 0.03)$  s.

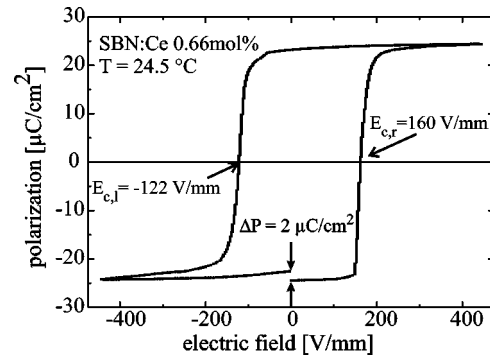


FIG. 4. Ferroelectric hysteresis loop in SBN:Ce (0.66 mol %) measured with a step height of  $\Delta E=3$  V/mm. Measuring frequency was  $3.4 \times 10^{-6}$  Hz. The measurement gives the expected values of coercive field (160 and  $-122$  V/mm) and spontaneous polarization [ $(23.7 \pm 1.0) \mu\text{C}/\text{cm}^2$ ].

to the value obtained for the first repoling process, and  $\beta=0.146 \pm 0.004$ , which is significantly lower than the corresponding one.

An even greater difference was observed when the electric field was removed. The polarization decay is now about five times larger and shows a considerably slower temporal behavior than the other decay measurements. This is also reflected in the fitting parameters obtained from this measurement. We derived  $\tau=(111 \pm 4)$  s, compared to  $\tau=0.02$  s for the first and  $\tau=8.5$  s for the second polarization decay. The parameter  $\beta$  can be fitted to  $0.145 \pm 0.004$  and differs significantly from those obtained for the first and second decay, but is identical to the corresponding value for the second repoling process.

### A. Ferroelectric hysteresis loops

Knowing the time behavior of the ferroelectric domains and the characteristic points of the hysteresis, we can analyze the frequency dependence of the whole hysteresis loop in order to get the response of the polarization to different external fields. Figure 4 shows the hysteresis loop of a SBN crystal doped with 0.66 mol % cerium at  $24.5^\circ\text{C}$ . The loop was measured in steps of  $\Delta E=3$  V/mm and widths of one minute for low external fields and up to 30 min in the vicinity of the coercive field. These steps have been long enough for the stabilization of the polarization in the external electric field to take place. The different step widths resulted in a total measuring time of about 82 h corresponding to a frequency of  $3.4 \times 10^{-6}$  Hz. Since the method is sensitive to changes in polarization, the absolute values of polarization are found by halving the distance between the first polarization reversal process at 0 V/mm and the maximum value at 450 V/mm. The result of the measurement is a typical hysteresis loop, showing the expected values of spontaneous polarization  $(23.7 \pm 1) \mu\text{C}/\text{cm}^2$ . The coercive field is asymmetric; on the right-hand side a value of  $(160 \pm 3)$  V/mm has been found, while the left gave  $(-122 \pm 3)$  V/mm. Near the coercive field the hysteresis curve is very steep, indicating an abrupt change of the domain orientation. For electric fields larger than 350 V/mm the curve is nearly lin-

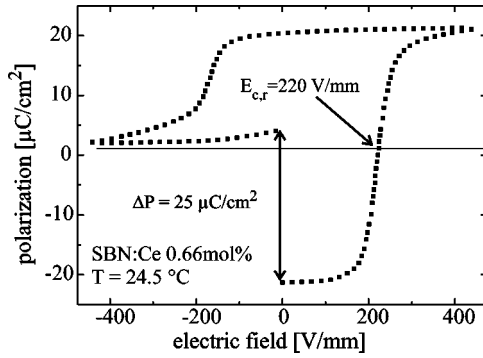


FIG. 5. Ferroelectric hysteresis loop of SBN:Ce (0.66 mol %) measured with a frequency of  $2.5 \times 10^{-4}$  Hz. The measurement was performed at a temperature of  $24.5$  °C. The coercive field is increased due to the inertia of the domains. The spontaneous polarization reaches the expected value of  $(22.0 \pm 1.0)$   $\mu\text{C}/\text{cm}^2$  on the right-hand side. The switching of the domains is incomplete on the left-hand side, resulting in a lower change of the polarization.

ear, indicating that all domains have switched their orientation and are now aligned in the direction of the external field. A similar behavior is observed on the left-hand side of the hysteresis curve, although the curve is not as steep as on the right-hand side. Furthermore, the hysteresis curve between  $-450$  and  $0$  V/mm is not a straight line, as it is on the right-hand side, but it shows a slight upward curvature at low electric fields. As a result the hysteresis curve is not totally closed and has a slight offset of  $\Delta P = 2.0$   $\mu\text{C}/\text{cm}^2$  at  $0$  V/mm.

We performed measurements with higher frequencies to find the origin of this anomaly. Fig. 5 shows such a hysteresis loop of the same SBN crystal doped with 0.66 mol % cerium, but measured with a step height of  $2.24$  V/mm and a width of  $5$  s, corresponding to a frequency of  $2.5 \times 10^{-4}$  Hz. The right flank of the hysteresis loop shows a spontaneous polarization of  $(22 \pm 1)$   $\mu\text{C}/\text{cm}^2$ , in agreement with the low-frequency measurement within error. However, the coercive field has a value of  $(220 \pm 5)$  V/mm. Further, the measured loop is not closed because the second polarization reversal renders much smaller values of surface-charge change and thus much smaller polarization values. We performed more cycles immediately after the first one since the state reached after one cycle is not stable. The results of the first, second, and tenth measurements are shown in Fig. 6. The data points are thinned out again. It can be seen that the second hysteresis loop is noticeably flatter and more smeared than the first, and it is still not closed. The next few cycles are omitted in the figure for reasons of lucidity, but the observed process continues at a slowing pace until a final state is reached after about five cycles. This final state is depicted in the 10th measurement as shown in the figure. This loop is closed, but the spontaneous polarization of  $(4.0 \pm 0.5)$   $\mu\text{C}/\text{cm}^2$  is only about 18% of the starting value.

To investigate the influence of the doping on the aging process, the hysteresis loops were also measured in a SBN crystal doped with 1.13 mol % cerium at  $24.7$  °C. The right flank of the first curve is again very steep and reaches a spontaneous polarization of  $(21 \pm 1)$   $\mu\text{C}/\text{cm}^2$  as reported

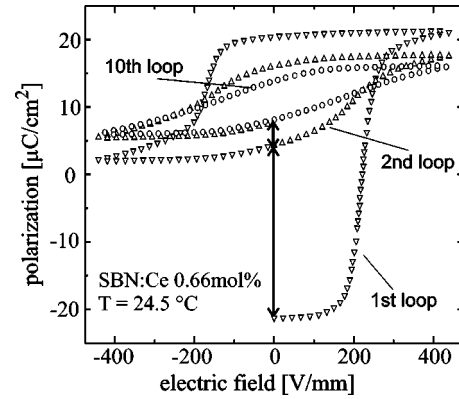


FIG. 6. First, second, and tenth hysteresis loop in SBN:Ce (0.66 mol %) at  $24.5$  °C; the decrease of the hysteresis that was observed in Fig. 5 continues at a slowing rate, until a final state is reached.

recently<sup>2</sup> and has a coercive field of  $(180 \pm 5)$  V/mm. As in the previous sample the first loop is not closed. The second polarization reversal causes much less change in polarization than the first, so that an aging process is observed again. After about seven cycles a stable closed hysteresis loop is reached. The final state shows a spontaneous polarization of  $(6.1 \pm 0.5)$   $\mu\text{C}/\text{cm}^2$ , which is about 28% of the original value. Therefore, the higher cerium doping leads to an aging process that takes even longer to finish and is not as pronounced as in SBN61 with lower dopant concentration.

The hysteresis loops were measured at different temperatures, too, to examine the temperature dependence of this polarization loss. Figure 7 shows exemplarily the experimental results of the SBN crystal doped with 0.66 mol % cerium and measured at  $T = 43.7$  °C. This temperature is close to the phase transition temperature of  $54$  °C. The measurement was realized with the same parameters as in Fig. 5. After the first cycle the flank with a spontaneous polarization of  $(18.6 \pm 1)$   $\mu\text{C}/\text{cm}^2$  becomes subsequently flatter, until a final state is reached after nine cycles. This final state has a spontaneous polarization of  $(7.1 \pm 0.5)$   $\mu\text{C}/\text{cm}^2$ , about 38% of the original value. That means the aging process progresses even more slowly at this higher temperature.

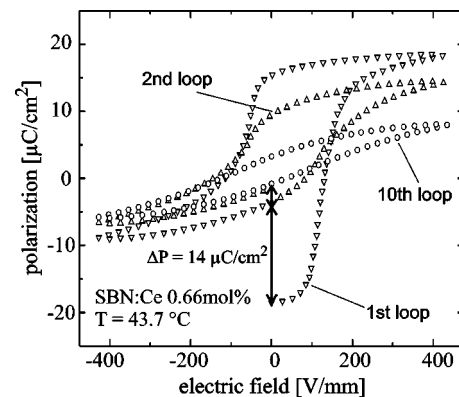


FIG. 7. First, second, and tenth hysteresis loop in SBN:Ce (0.66 mol %) at  $43.7$  °C. The higher temperature results in an even slower aging process.



#### IV. DISCUSSION

The results unambiguously show that an electrical aging of both the temporal behavior of the polarization and the ferroelectric hysteresis loops takes place in SBN61 crystals doped with cerium. This effect has so far been observed in high-frequency measurements and experiments with thin films and structurally imperfect crystals<sup>10,11</sup> only.

##### A. Temporal behavior of domain walls and the polarization reversal

Figures 1 and 2 clearly show that the field-cooled crystal is nearly completely poled, since the polarization does not change significantly when an electric field is applied in the direction of the prepared polarization. 90% of the small observed change of  $0.53 \mu\text{C}/\text{cm}^2$  can be attributed to the static dielectric constant of  $\epsilon_{33}=1840$ . This indicates that this buildup of polarization is predominantly caused by the static dielectric constant, but not by the behavior of the ferroelectric domains. The remaining 10%, about  $55 \text{ nC}/\text{cm}^2$ , can be assigned to small ferroelectric domains. This amount of polarization is negligible compared to the total spontaneous polarization of  $23.7 \mu\text{C}/\text{cm}^2$ . When the electric field is removed, the polarization drops back by the same amount, thus returning the sample to its original polarization state. The first two figures therefore evidence that cooling the crystal in an external electric field results in a nearly stable configuration in which all the domains are aligned. This configuration does not decay on a time scale of several days, even without stabilization of an external field.

The fact that fitting with the KWW function yields good results allows two different interpretations: Either the dynamics of the ferroelectric domains are inherently nonexponential as a consequence of strong interactions between the domains, or the observed behavior results from a superposition of many different relaxation times of independently relaxing domains. For all systems examined so far showing a net nonexponential behavior, the second assumption proves to be correct: The KWW-like behavior with values of  $\beta \leq 1$  is caused by a superposition of numerous single exponentials with different time constants.<sup>15</sup> Lower values of  $\beta$  for the same value of  $\tau$  also indicate a slower behavior for large times. The time constant  $\tau$  is not *the* decay time of all ferroelectric domains, but signifies the range where most of the single decay times lie. It has been shown that a KWW-like behavior can be attributed to a system where the relaxation time of a single domain depends on its size: The larger the domain, the longer it takes to reverse its polarization.<sup>16,17</sup> This is the low-temperature approximation of Chamberlin's theory of dynamically correlated domains (DCD's),<sup>18</sup> which has successfully been applied to various relaxor ferroelectric compounds.<sup>19,20</sup> We therefore base the following discussion on this model of size-dependent domain relaxation times.

The first repoling process shown in Fig. 3 is very fast and gives values of the polarization in the same order of magnitude as the ferroelectric hysteresis. This shows that all the domains are switched with the external electric field. The difference of  $1.7 \mu\text{C}/\text{cm}^2$  is due to the limited time resolution of our charge amplifier. The polarization change directly

after the application of the electric field is too fast and cannot be detected completely. The clearly linear behavior for  $42 \geq t \geq 14 \text{ h}$  shows that only the dark current contributes to the surface-charge change at this time scale, where the domain dynamics are no longer operating.

The value of  $\beta=0.4$  shows that the system cannot be described with one or two exponential functions. This means there is neither a single switching time, nor a superposition of two or three different time constants, but there are many different switching times present in the system. Since the switching time of a domain is supposed to depend on the domain size, this is a clear sign that the size distribution of the domains is very broad. The value of  $\tau=1.99 \text{ s}$  is much larger than the ones in Figs. 1 and 2. This shows that the dynamics of the ferroelectric domains are still quite fast, but considerably slower than the first poling and depoling process.

The decrease of the electric polarization after this first repoling process is slightly larger than the one observed before repoling, and it also takes slightly longer.  $\beta$  is again very small, an indication that this decay of the polarization is still dominated by normal dielectric behavior, not by the dynamics of the ferroelectric domains. This means that the ferroelectric domains are nearly as stable as the configuration observed immediately after the FC process.

The first real indication of an electrical aging of the material becomes prominent in the subsequent second repoling process, where only a small fraction of the ferroelectric domains is switched during the time of the measurement. The  $P(t)$  curve does not reach a saturated state after more than 56 h, indicating that a very slow polarization reversal process is still active even after several days. The small value of  $\beta$ , combined with the relatively large value of  $\tau$ , supports this conclusion.  $\beta=0.146$  shows that the ferroelectric domains do not switch with a common switching time, but that the distribution of switching times and therefore domain sizes is even wider than before. When the electric field is removed, it becomes obvious that the state reached is not very stable. A polarization decrease by  $2.8 \mu\text{C}/\text{cm}^2$ , nearly five times as large as the ones observed before, takes place. This decay process occurs on a very long time scale; it is not finished after more than 30 h. Once again, this is reflected in the large value of  $\tau=111 \text{ s}$ . The value of  $\beta$  is comparable to the one observed in the second repoling process. This indicates that the size distribution of the domains has not changed much between the process of polarization buildup and decay.

##### B. Ferroelectric hysteresis loops

Figure 4 shows that a measurement with a very low frequency results in a hysteresis curve that is nearly rectangular and almost closed. This proves that the used method of quasistatic surface-charge detection is applicable not only for the measurement of static electric polarization, but also for measurements of low-frequency hysteresis loops. The known values of the spontaneous polarization could be reproduced. Other effects that cause charge carriers to appear on the crystal surface, such as dark currents through the crystal, play only a minor role and do not influence the results signifi-

cantly. The coercive field is asymmetric. This is an effect of the primary poling process, that clearly caused a preferred direction of the domains. Since the coercive field is higher on the right-hand side than on the left-hand side, it seems to be more difficult to switch the orientation of the domains they achieved at high temperatures, but easy to switch them back again. The potential well of the domains is clearly asymmetric due to the field-cooling process. The small discrepancy in the polarization at 0 V/mm indicates that even a frequency of  $10^{-6}$  Hz, equivalent to a measuring time of four days, is not low enough to suppress electrical aging completely. However, the hysteresis curve is clearly saturated at electric fields above 350 V/mm, so that effects like minor hysteresis loops, i.e., loops that are measured with too-low field amplitudes, can be excluded in the further discussion of the electrical aging process.

The fact that the right-hand flank of the hysteresis loop shown in Fig. 5 is nearly rectangular and shows saturation for high electric fields indicates that all ferroelectric domains are completely switched during this first repoling process. This behavior corresponds very well with the observations made for the quasistatic  $P(t)$  measurement shown in Fig. 3. The coercive field appears to be significantly higher at this higher frequency. This can directly be explained by the dynamics of the ferroelectric domains. Domains do not switch instantaneously, but need a certain time to reverse their orientation. There is not enough time in the high-frequency measurement for the domains to stabilize in the externally applied electric field. This causes a lag between the electric field and the electric polarization, and thus the coercive field seems to shift to higher values. However, the switching process is clearly finished at fields exceeding 350 V/mm. In contrast, only a fraction of the domains is switched during the second repoling process. This is the same behavior that was already observed in the measurement with constant external field. In both cases, the polarization does not follow the external electric field, but shows a pronounced slowing down. We assume that the domains themselves are not the reason for this sluggishness, as they are able to follow the first repoling process at high frequencies (Figs. 3 and 5). For a better understanding of this behavior we have to discuss the process of domain-orientation reversal first.

### C. Domain-orientation reversal and pinning centers

The orientation of the ferroelectric domains is reversed by the formation of small areas with polarization antiparallel to the predominant polarization direction.<sup>21,22</sup> These areas are called nuclei and form in the vicinity of the electrodes. They expand into the bulk of the crystal by motion of the domain walls. The walls of the nucleus travel through the crystal bulk, changing the orientation of the microscopic polarization in the areas in which they trespass.<sup>23</sup> This leads to the formation of needle-shaped domains, since the domain walls propagate mainly in the direction of the crystallographic  $c$  axis.<sup>7,24</sup> Reduction of the change in polarization can have two causes: prevention of nucleation of reversely poled microdomains or hindrance of the domain-wall motion. Prevention of nucleation has to be excluded, since more than 80%

of the crystal surface has to change for the observed decrease of the hysteresis loops. Changes of such large crystal surface areas could not have gone unnoticed in other experiments such as holographic scattering. Now, let us discuss the reduction of the polarization change by hindrance of the domain-wall motion. Domain walls can be hindered in their motion by certain defects in the crystal structure.<sup>25,26</sup> This effect is called ‘‘pinning’’ and has been observed in SBN with different methods, e.g., atomic force microscopy<sup>27</sup> and holographic two-beam coupling.<sup>28</sup> The nature of the pinning centers can also be deduced by the behavior of the hysteresis loops. All crystals show a strong anisotropy with respect to the orientation of the polarization. The orientation of the domains that is antiparallel to the direction of the electric field during the poling process is preferred. One can overcome this preference at room temperature using high electric fields that are applied for a sufficiently long time, as shown in Fig. 4. However, the applied fields are not large enough to change the crystal structure itself. Since the effects of aging can be reversed by waiting long enough, it is reasonable to assume that this pinning is not caused by crystal defects but by electric fields. Such fields may be produced by fluctuations of the local ionic charges, caused, e.g., by the holes in the unfilled tungsten-bronze structure. During sample preparation at high temperatures these fluctuations are highly mobile, and their dynamics are dominated by the externally applied electric field. After cooling down in the electric field the fluctuations are frozen, leading to ‘‘quenched random fields,’’ a necessary assumption in a ‘‘random-field Ising model’’ as proposed by Kleemann.<sup>13,19</sup> These random fields stabilize the domain walls after the first switching of the polarization. Once the domain walls are pinned, the domain-switching mechanism is suppressed. The polarization in the crystal bulk no longer changes its orientation in an external electric field. This causes the observed aging effect. Higher concentrations of cerium raise the dark conductivity of the material, as does high temperature. Higher conductivity allows free charge carriers to compensate the quenched random fields, leading to a slower aging process, as shown in Fig. 7. If the frequency of the measuring cycle is low enough, the ‘‘stopping power’’ of the pinning centers is eventually overcome by the domain walls, resulting in the nearly closed hysteresis loop shown in Fig. 4. The time dependence of the domain switching and polarization decay is a further indication of a ‘‘random-field Ising model.’’ The  $P(t)$  curves can very well be fitted with a stretched exponential function. This function is the low-temperature approximation of the so-called ‘‘DCD function,’’ which has been shown to describe the behavior of dynamically correlated domains.<sup>16</sup> This behavior is the key to the understanding of relaxor behavior at higher temperatures.

The observed parameters  $\beta$  and  $\tau$  entering the KWW-type relaxation law, Eq. (1), are in accordance with the corresponding parameters emerging from DCD-type response functions fitted to ac susceptibility data.<sup>14</sup> At room temperature, unpoled (ZFC) SBN61:Ce reveals extremely large (negative) correlation coefficients,  $C \approx -500$ , while  $C \approx -10$  in the poled (field-cooled) state. Within the DCD theory<sup>15</sup> such values refer to extremely large (ZFC) and

weak (field-cooled) polydispersivity, as expressed, conversely, by very small ( $\approx 0.05$ ) and intermediate ( $\approx 0.5$ )  $\beta$  values, respectively, in the KWW approach.

Physically these extreme differences can be understood as follows: Upon zero-field cooling the system decays into an extremely fine-grained domain state, where the domains are trapped in well-defined and optimized local free-energy minima. Hence, a very wide distribution of relaxation rates can be expected. On the other hand, after FC, the system refers to a quasisingle domain state that has an enhanced free energy due to averaging over the potential landscape of quenched random fields with either sign. When reorienting this state by virtue of an electric field with opposite sign, the energy barriers to overcome are shallower than in the ZFC state. This reduces the polydispersivity by an appreciable amount, as reflected by high  $\beta$  and low  $|C|$  values. Finally, the average KWW lifetimes,  $\tau(\text{ZFC}) \approx 10^{-2}$  s and  $\tau(\text{field cooled}) \approx 10^0 - 10^2$  s, account for the different average domain sizes in different states. While small domains with low activation energies prevail in the ZFC state, the larger field-cooled domains require longer attempt times for reorientation.

It is important to understand that the fluctuations of the electric field in the crystal bulk are only weak effects. The stable hysteresis loops at higher frequencies are nearly symmetric, so that the fluctuations are by no means strong enough to influence entire domains or form a macroscopic bias field in the crystal. It is not necessary to macroscopically influence electric fields in order to change the ferroelectric hysteresis, as microscopic disturbances located at the domain wall are sufficient to prevent the switching of the whole domain.

#### ACKNOWLEDGMENTS

This work was supported by the Deutsche Forschungsgemeinschaft within the framework of the Schwerpunktprogramm SPP 1056: ‘‘Strukturgradienten in Kristallen’’ (Projekt WO 618/3-2). Theo Woike is very indebted to the University of Nancy (Institute of Crystallography) for his stay as a guest professor and the fruitful discussions with N.K. Hansen, V. Petricek, P. Fert, and C. Lecomte.

- 
- <sup>1</sup>A.M. Glass, *J. Appl. Phys.* **40**, 4699 (1969).  
<sup>2</sup>T. Woike, T. Volk, U. Dörfler, R. Pankrath, L. Ivleva, and M. Wöhlecke, *Ferroelectr. Lett. Sect.* **23**, 127 (1998).  
<sup>3</sup>U.B. Dörfler, R. Piechatzek, Th. Woike, M.K. Imlau, V. Wirth, L. Bohat, T. Volk, R. Pankrath, and M. Wöhlecke, *Appl. Phys. B: Laser Opt.* **68**, 843 (1999).  
<sup>4</sup>P.B. Jamieson, S.C. Abrahams, and J.L. Bernstein, *J. Chem. Phys.* **48**, 5048 (1968).  
<sup>5</sup>L.E. Cross, *Ferroelectrics* **76**, 241 (1987).  
<sup>6</sup>W.H. Huang, D.C. Viehland, and R.R. Neurgaonkar, *J. Appl. Phys.* **76**, 490 (1994).  
<sup>7</sup>H. Arndt, T.V. Dung, and G. Schmidt, *Ferroelectrics* **97**, 247 (1989).  
<sup>8</sup>P. Lehnen, W. Kleemann, Th. Woike, and R. Pankrath, *Eur. Phys. J. B* **14**, 633 (2000).  
<sup>9</sup>L.A. Bursill and P.J. Lin, *Acta Crystallogr., Sect. A: Found. Crystallogr.* **43**, 49 (1987).  
<sup>10</sup>R.B. Maciulek and S.T. Liu, *J. Electron. Mater.* **2**, 191 (1973).  
<sup>11</sup>B. Jimenez, C. Alemany, J. Mendiola, and E. Maurer, *Ferroelectrics* **38**, 841 (1981).  
<sup>12</sup>H.R. Xia, C.J. Wang, H. Yu, H.C. Chen, and Y.Y. Song, *Cryst. Res. Technol.* **31**, 889 (1996).  
<sup>13</sup>W. Kleemann, *Phase Transitions* **65**, 141 (1998).  
<sup>14</sup>J. Dec, W. Kleemann, Th. Woike, and R. Pankrath, *Eur. Phys. J. B* **14**, 627 (2000).  
<sup>15</sup>R.V. Chamberlin, *Phase Transitions* **65**, 169 (1998).  
<sup>16</sup>R.V. Chamberlin and D.N. Haines, *Phys. Rev. Lett.* **65**, 2197 (1990).  
<sup>17</sup>R.V. Chamberlin, *Europhys. Lett.* **33**, 545 (1996).  
<sup>18</sup>R.V. Chamberlin, *Phys. Rev. B* **48**, 15 638 (1993).  
<sup>19</sup>W. Kleemann, *J. Korean Phys. Soc.* **32**, 939 (1998).  
<sup>20</sup>W. Kleemann, A. Albertini, R.V. Chamberlin, and J.G. Bednorz, *Europhys. Lett.* **37**, 145 (1997).  
<sup>21</sup>L.I. Dontsova, N.A. Tikhomirova, and L.A. Shuvalov, *Crystallogr. Rep.* **39**, 140 (1994).  
<sup>22</sup>Y. Ishibashi and Y. Takagi, *J. Phys. Soc. Jpn.* **31**, 506 (1971).  
<sup>23</sup>V. Gopalan and T.E. Mitchell, *J. Appl. Phys.* **83**, 941 (1998).  
<sup>24</sup>V. Grubsky, S. MacCormack, and J. Feinberg, *Opt. Lett.* **21**, 6 (1996).  
<sup>25</sup>T. Nattermann, Y. Shapir, and I. Vilfan, *Phys. Rev. B* **42**, 8577 (1990).  
<sup>26</sup>W.L. Warren, D. Dimos, B.A. Tuttle, R.D. Nasby, and G.E. Pike, *Appl. Phys. Lett.* **65**, 1018 (1994).  
<sup>27</sup>Y.G. Wang, W. Kleemann, Th. Woike, and R. Pankrath, *Phys. Rev. B* **61**, 3333 (2000).  
<sup>28</sup>U. Dörfler, M. Imlau, Th. Woike, W. Kleemann, R. Pankrath, and M. Wöhlecke, *Z. Kristallogr. - New Cryst. Struct.* **S17**, 217 (2000).